Field dependency of magnetoelectric coupling in multilayered nanocomposite arrays: Possible contribution from surface spins

Xiaoli Lu,^{1,a)} Sining Dong,² Xiaoguang Li,² Marin Alexe,³ Dietrich Hesse,³ and Yue Hao^{1,b)} ¹State Key Discipline Laboratory of Wide Band Gap Semiconductor Technology, School of Microelectronics, Xidian University, 710071 Xi'an, China

(Received 12 August 2012; accepted 6 November 2012; published online 27 November 2012)

Highly ordered BaTiO₃/CoFe₂O₄ (BTO/CFO) epitaxial heterostructures were grown via modified stencil-assisted pulsed laser deposition. With proper particle size and good crystal quality, the magnetoelectric (ME) coupling effect of the as-prepared nanodots can be probed in a low field. Unexpected coupling relaxation was found after BTO phase transition onset in low field (50 Oe) but was suppressed in high field (50 kOe). This field dependency of ME coupling is proposed to originate in different contributions from bulk and disordered surface spins. The results may provide a way to enhance ME coupling at nanoscale for the design of low-field operated multifunctional ME devices. © 2012 American Institute of Physics. [http://dx.doi.org/10.1063/1.4768290]

As choice for voltage-driven magnetic recording devices, magnetoelectric (ME) materials hold the promise to be suitable for next-generation memories with high storage capacity, ultrafast access speed, low-energy dissipation, and non-volatility. To fulfill this promise, the bottleneck problem is to find proper materials showing sizable room-temperature ME coupling at low field. Since natural single-phase systems rarely show a prominent room-temperature ME effect, great effort had been devoted to the design and fabrication of ME composites in recent years. Various ferroelectric and magnetic materials were combined in such composites. Elastic interaction, i.e., interfacial strain, mediates the ME coupling, which was proven to effectively enhance the ME response up to 310 V cm⁻¹ Oe⁻¹.

With the actual trend of device integration, nanostructured ME composites receive more and more attention. Different from their bulk counterparts, as size decreases, other interfacial characteristics such as charge carriers, exchangebias, chemical bonding, etc., can also make an important contribution to the ME effect. In these cases, more physical phenomena will arise from these coupling factors and help to obtain a better understanding of the ME behavior. But ME coupling in nanocomposites (NCs) has been less well explored due to many challenges beyond microscopic and systematic studies, such as the precise control of lattice matching, connectivity order and dimension of each part in the composite.

With the advances in epitaxy techniques, multilayered thin films, i.e., 2-2 NCs, were subject to intensive investigations; different phases were combined at atomic level with near-perfect mechanical coupling, but the ME response is limited to quite a low level due to clamping from the stiff substrate. Ramesh *et al.* developed nanostructured self-assembled vertical epitaxial columnar films, i.e., 1-3 (or 3-1) NCs, and opened a way to reduce substrate clamping and maintain interfacial strain.⁶ A significant enhancement of ME coupling, and electric-field induced magnetization

switching, was achieved in 1-3 NCs. Further applications of 1-3 NCs were hindered, however, by their uncontrollable component distribution and limited choice of materials; it is not trivial to solve these problems due to the self-assembly nature of the preparation process. Recently, Lu *et al.* proposed epitaxial multilayered nanodot arrays, i.e., 0-0 NCs via a stencil assisted direct epitaxy process. It was designed to combine the features of 2-2 and 1-3 structures with good control of component assembly and confined lateral size to reduce substrate clamping. A clear coupling effect was found in these tiny nanodots (less than 60 nm in thickness), indicating great potential as a model system for further investigation of ME materials and for making device prototypes.

In the previous report, BaTiO₃/CoFe₂O₄ (BTO/CFO) heterostructured nanodots (consisting of up to 4 layers) were fabricated as a test system to study 0-0 NCs. Phase transitioninduced strain in BTO was found to result in a magnetization anomaly (ΔM) in the CFO layer, which was ascribed to be the signature of an effective ME coupling in these nanodots. For stencil-assisted pulsed laser deposition (PLD), good epitaxial quality relies on the proper choice of stencil and oxygen pressure. Normally, a larger aspect ratio (AR, thickness-to-pore diameter ratio) requires a lower oxygen pressure (P_{O2}) for deposition through the stencil channels.¹⁰ Insufficient oxygen (low P_{O2}) may, however, introduce many defects and reduce the crystal quality. For the BTO/CFO nanodots in Ref. 9, oxalic acid-derived anodic aluminum oxide (AAO) membranes (AR $\sim\!2)$ were used as contact mask, which enabled the deposition in $P_{\rm O2}$ of $10^{-2}\,\rm Torr.$ Highly ordered epitaxial nanocomposite (diameter ~65 nm) arrays with up to 4 layers were fabricated. But further increase of the number of composite layers and of thickness failed due to the limitation of mask AR and pore closing effect. 10 With such tiny amount of materials, the ME coupling of as-prepared BTO/CFO nanodots was investigated in a relatively high probe field (50 kOe) due to measurement limitations, so that the ME coupling signal can be somewhat enlarged. But many other effects may also be hidden in such a high magnetic field.

²Hefei National Laboratory for Physical Sciences at Microscale, Department of Physics, University of Science and Technology of China, Hefei 230026, China

³Max Planck Institute of Microstructure Physics, 06120 Halle (Saale), Germany

a)Electronic mail: xllu@live.cn.

b)Electronic mail: yhao@xidian.edu.cn.

In this letter, a modified stencil was used for the deposition. BTO/CFO nanodots with better crystal quality and bigger size were fabricated, enabling a low-field investigation of the ME effect. Unexpected coupling relaxation was found, which can be suppressed with high field. This field dependency of the ME coupling was ascribed to different contributions from bulk and surface spins. These results may help to shed light on the origin of ME effects at nanoscale and provide references for the study of low-field operated ME devices.

Phosphoric acid (H₃PO₄) derived AAO membrane (twostep anodization at 195 V dc voltage in 0 °C 1 wt. % H₃PO₄) was chosen as stencil mask here; the mask AR was confined as low as possible (AR \sim 1) to enable the following deposition at the same oxygen pressure as that used for normal thin film growth (around 0.1 Torr). The mask was then transferred to a (001) SrTiO₃ (STO) single crystal substrate (5 mm \times 5 mm \times 0.5 mm in dimension) provided with an epitaxial SrRuO₃ bottom electrode layer. BTO and CFO were subsequently deposited through the AAO mask at $T \sim 650$ °C, $P_{\rm O2} \sim 10^{-1} \, {\rm Torr}, \ {\rm f} \sim 5 \, {\rm Hz}, \ {\rm and} \ {\rm E} \sim 0.7 - 0.9 \, {\rm J \ cm}^{-2} \ {\rm via} \ {\rm PLD}$ (KrF excimer laser, $\lambda = 248 \text{ nm}$) to obtain a 4-layered structure. The mask confined the growth and hexagonally ordered nanodot arrays with a dot diameter around 350 nm were formed [as shown in Fig. 1(a)]. To check the crystallographic and epitaxial quality of the as-prepared nanodots, X-ray diffraction (XRD) patterns were collected on a commercial diffractometer (Philips X'Pert MRD) with Cu Kα instead of synchrotron radiation, which is normally used for nanodot arrays with small particle size. ¹⁰ Figure 1(b) shows the θ –2 θ diffraction patterns for the nanodots, which display clear peaks from (0 0 2) planes of STO, and broad (0 0 l) peaks of BTO and CFO. An in plane 360° Φ scan was also performed using the $(l \ l \ 0)$ peaks [Fig. 1(c)], indicating the coherent growth of each layer.

High resolution transmission electron microscopy (HRTEM) was then used to obtain more local information on the interfaces in these nanodots. As shown in Fig. 1(d)), a randomly selected nanodot was sectioned by a standard focused-ion-beam technique, and characterized in cross section. As expected, clear lattice images in Fig. 1(e) show stacked layer structures of around 15 nm individual layer thickness. According to the fabrication sequence, these layers should be BTO/CFO/BTO/CFO epitaxial nanodots, and this was confirmed by a corresponding fast Fourier transform (FFT) in Fig. 1(f). The inverse FFT image in Fig. 1(g) shows the filtered HRTEM information from selected planes, where a nice epitaxial stacking of BTO (200) and CFO (400) planes can be seen much more clearly. These atomically sharp interfaces form the basis for an effective ME coupling in the BTO/CFO nanodots.

As a ferrimagnetic material with a large magnetostrictive effect, CFO was found to be very sensitive to strain, which can induce changes in magnetization, magnetic anisotropy, and so on. With size reducing, surface anisotropy, spin canting, exchange bias, etc., become more and more important for CFO magnetism, a combination of these factors possibly enhancing the ME coupling in composites. 14

As inspired by the structure analysis above, especially the XRD data, good crystal quality and large particle size might make the ME response of as-obtained nanodots strong enough to be detected in a low probe field. The room temperature in-plane magnetization vs. external field (*M-H*) curve was collected on a superconducting quantum interference device (SQUID). Here, a clear hysteresis loop with a coercive field (*Hc*) around 150 Oe was recorded [Fig. 2(a)]. There is a paramagnetic like non-saturating part (the linear part) in the *M-H* curve, indicating a considerable contribution from disordered surface spins in the sample. ¹⁵ To check the ME effect in the sample, a magnetization vs temperature

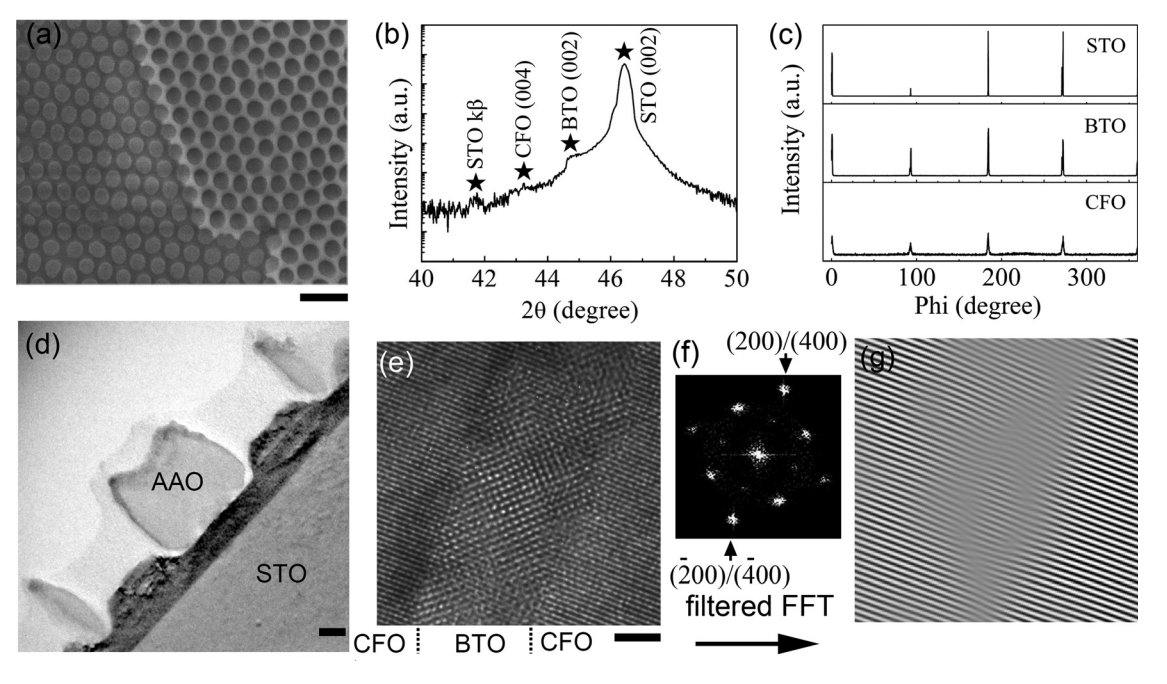


FIG. 1. (a) Field emission scanning electron micrograph (FESEM) of as-prepared BTO/CFO nanodot arrays; XRD study: (b) θ -2 θ scan and (c) Φ scan in (l l 0) planes; HRTEM results: (d) bird-eye view of as-obtained nanodots and AAO mask, (e) high resolution crystal lattice and (f) corresponding FFT image, (g) filtered HRTEM image of BTO (200) and CFO (400) planes; Scale bars: (a) $1000 \, \text{nm}$, (d) $100 \, \text{nm}$, and (e) $5 \, \text{nm}$.

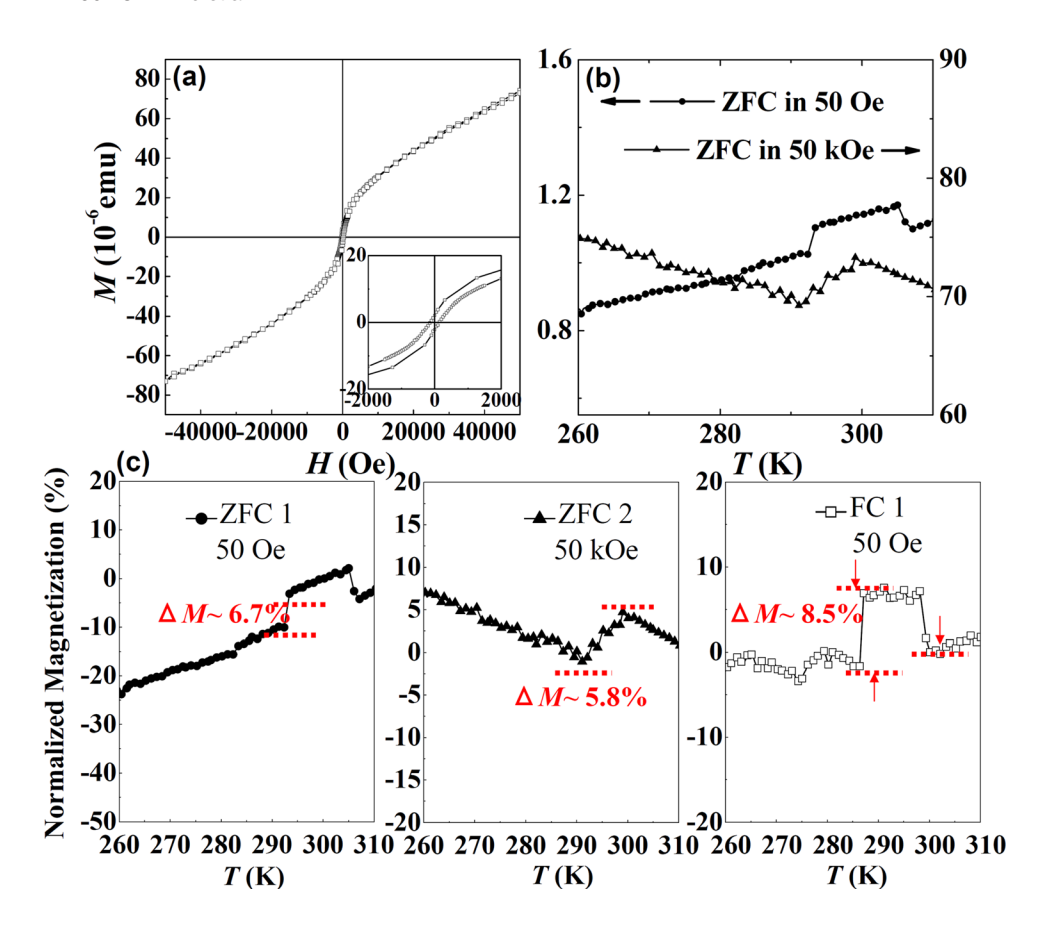


FIG. 2. SQUID study of BTO/CFO nanodots: (a) room temperature *M-H* curve; the inset is an enlarged view around the origin, (b) in-plane ZFC curves in 50 Oe and 50 kOe magnetic field, (c) comparison of probe field-induced and poling process-induced different ME coupling.

(M-T) curve was investigated across the BTO tetragonal-toorthorhombic phase transition temperature (T to O, \sim 290 K), where a crystallographically induced strain will be transferred to the CFO and affects M. The sample was cooled down to 260 K in zero field, and M was measured in a 50 Oe probe field with the temperature ramping up to 310 K [ZFC 1, Fig. 2(b)]. As expected, an anomaly in $M(\Delta M)$ was found around 292 K, which can be attributed to the increase of the compressional strain in CFO.¹⁷ In contrast to the bulk CFO, the M in ZFC1 decreases with decreasing temperature, which could be due to the disordered surface spin or the diamagnetism from the BTO substrate. The ΔM unexpectedly relaxes to the normal value at around 306 K, leaving a pulse-like kink in the *M-T* curve. For comparison, an *M-T* curve [ZFC 2, Fig. 2(b)] in a high probe field (50 kOe) was also measured, where a distinct M change around 290 K was found, too, but no relaxation behavior showed up this time.

These different ME responses indicate a field-dependent coupling effect in the nanodots. It was reported that strain can be relaxed sideways in nanoislands, ¹⁸ thus, this ΔM relaxation could be a consequence of strain relaxation. But the induced strain in BTO is not field sensitive; in this case, a similar relaxation in M should also be found in ZFC2. Thus, another mechanism should be responsible for the coupling. According to the M-H curve above, disordered surface spins which can be partially aligned in the high field might provide a clue. To check this idea, another M-T curve (FC 1) was measured with the sample cooled down to 260 K in a field of 50 kOe ("poling process"), and the M signal was collected during temperature ramping in a probe field of 50 Oe. For better comparison, three M-T curves were all normalized to the magnetization at 300 K and aligned in

Fig. 2(c). Different from ZFC 1, there is an enhancement of ΔM in FC 1 around 290 K, and, even more interestingly, ΔM in FC 1 did not fully relax after the BTO phase transition, leaving a small part of residual increase as marked by arrows in Fig. 2(c). The enhancement and non-relaxed part of ΔM in FC 1 all indicate that there might be a contribution of aligned surface spins to the ME coupling effect.

Based on these results, a simple explanation of the fielddependent ME coupling in as-prepared nanodots is proposed and schematically shown in Fig. 3. In fields lower than the bulk saturation field (Hs) of CFO nanodots, only part of bulk spins is aligned with the external field. When the BTO phase changes from O to T, a compressional strain is transferred to the CFO, which can induce more aligned bulk spins due to a reciprocal magnetostrictive effect leading to an M increase.¹⁹ This effect can be considered as a strain-induced extra field (He) applied to the sample, ²⁰ and this He is not big enough to align the surface disordered spins. So, in low field, only bulk spins contribute to the ΔM . When the external field is much higher than Hs, most bulk spins are already aligned; He will not further enlarge M. But since the field is high enough, disordered surface spins will now be partially aligned, so that He could affect these pre-aligned spins and induce a linear increase of M. Unlike bulk spins, ΔM from surface spins prefer to keep their original positions due to a pinning effect at the interface, 21 and ΔM can be maintained even after strain relaxation (He removed). Thus, in high field, the persistent part of ΔM should come from surface spins. In this context, a field cooled sample gaining a combination of bulk and surface spin-induced ME effect will show larger coupling. Actually, what really happened in the interface-mediated ME coupling could be more complicated

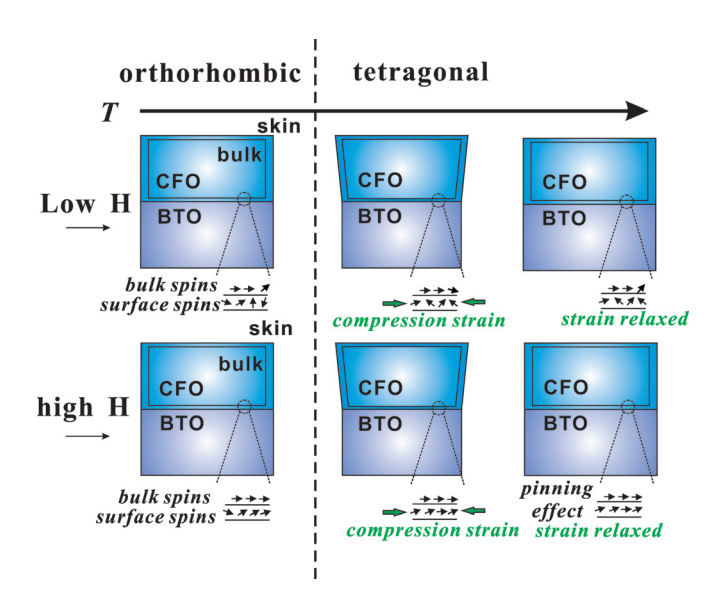


FIG. 3. Schematic illustration of different responses of bulk and surface spins in CFO nanodots across the BTO phase transition; the small black arrows indicate the direction of spin moments.

than this phenomenological explanation, and it is also impossible to obtain a detailed insight into the ME effect via only magnetization measurements. These well-organized nanodot arrays deserve more systematic investigations experimentally and theoretically. Our results have nevertheless revealed a ME coupling relaxation behavior at nanoscale and a possible pathway to enhance the ME coupling in nanocomposites.

In summary, high quality and well ordered BTO/CFO nanodot arrays were fabricated with optimized AAO stencils. An unexpected field-dependent ME effect was found in the as-prepared nanocomposite, where the low-field ME effect gradually relaxes with increasing temperature, while the high-field one maintains. A possible explanation regarding the different contribution from bulk and surface spins was proposed, based on which an enhanced ME coupling was found in high-field poled nanodots due to a combined ME effect. These results may provide reference for investigating

and optimizing the interface-derived ME effect at nanoscale for building low-field operated multifunctional ME devices.

The authors acknowledge German Science Foundation (DFG) for support via SFB 762, the Alexander von Humboldt foundation, and the support of NSFC (Contract Nos. 51202176 and 50832007) and the NBRPC (Contract No. 2012CB922003, X. G. Li).

¹J. Ma, J. Hu, Z. Li, and C.-W. Nan, Adv. Mater. 23, 1062 (2011).

²J. Zhai, S. Dong, Z. Xing, J. Li, and D. Viehland, Appl. Phys. Lett. **89**, 083507 (2006).

³H. J. A. Molegraaf, J. Hoffman, C. A. F. Vaz, S. Gariglio, D. van der Marel, C. H. Ahn, and J.-M. Triscone, Adv. Mater. **21**, 3470 (2009).

⁴A. Hochstrat, C. Binek, X. Chen, and W. Kleemann, J. Magn. Magn. Mater. **272–276**, 325 (2004).

⁵C. G. Duan, S. S. Jaswal, and E. Y. Tsymbal, Phys. Rev. Lett. **97**, 047201 (2006).

⁶H. Zheng, J. Wang, L. Mohaddes-Ardabili, M. Wuttig, L. Salamanca-Riba, D. G. Schlom, and R. Ramesh, Appl. Phys. Lett. **85**, 2035 (2004).

⁷F. Zavaliche, H. Zheng, L. Mohaddes-Ardabili, S. Y. Yang, Q. Zhan, P. Shafer, E. Reilly, R. Chopdekar, Y. Jia, P. Wright, D. G. Schlom, Y. Suzuki, and R. Ramesh, Nano Lett. 5, 1793 (2005).

⁸R. Ramesh and N. A. Spaldin, Nat. Mater. **6**, 21 (2007).

⁹X. L. Lu, Y. S. Kim, S. Goetze, X. G. Li, S. N. Dong, P. Werner, M. Alexe, and D. Hesse, Nano Lett. 11, 3202 (2011).

¹⁰W. Lee, H. Han, A. Lotnyk, M. A. Schubert, S. Senz, M. Alexe, D. Hesse, S. Baik, and U. Gosele, Nat. Nanotechnol. 3, 402 (2008).

¹¹W. Huang, J. Zhu, H. Z. Zeng, X. H. Wei, Y. Zhang, and Y. R. Li, Appl. Phys. Lett. **89**, 262506 (2006).

¹²X. S. Gao, D. H. Bao, B. Birajdar, T. Habisreuther, R. Mattheis, M. A. Schubert, M. Alexe, and D. Hesse, J. Phys. D: Appl. Phys. 42, 175006 (2009)

¹³A. T. Ngo, P. Bonville, and M. P. Pileni, J. Appl. Phys. **89**, 3370 (2001).

¹⁴C. A. F. Vaz, J. Hoffman, C. H. Anh, and R. Ramesh, Adv. Mater. 22, 2900 (2010).

¹⁵A. Mumtaz, K. Maaz, B. Janjua, S. K. Hasanain, and M. F. Bertino, J. Magn. Magn. Mater. 313, 266 (2007).

¹⁶M. K. Lee, T. K. Nath, C. B. Eom, M. C. Smoak, and F. Tsui, Appl. Phys. Lett. 77, 3547 (2000).

¹⁷R. V. Chopdekar and Y. Suzuki, Appl. Phys. Lett. **89**, 182506 (2006).

¹⁸F. Bertram, J. Christen, M. Schmidt, K. Hiramatsu, S. Kitamura, and N. Sawaki, Physica E 2, 552 (1998).

¹⁹J. A. Paulsen, A. P. Ring, C. C. H. Lo, J. E. Snyder, and D. C. Jiles, J. Appl. Phys. **97**, 044502 (2005).

²⁰J. Ryu, S. Priya, K. Uchino, and H. E. Kim, J. Electroceram. **8**, 107 (2002).

²¹J. Nogues and I. K. Schuller, J. Magn. Magn. Mater. **192**, 203 (1999).